

# METHOD FOR CALIBRATING THE IMAGE FROM A MIXEL CAMERA BASED SOLELY ON THE ACQUIRED HYPERSPECTRAL DATA

*Gudrun Høye, and Andrei Fridman*

Norsk Elektro Optikk, Lørenskog, Norway; [gudrunkh\(at\)alumni.ntnu.no](mailto:gudrunkh@alumni.ntnu.no), [fridman\(at\)neo.no](mailto:fridman(at)neo.no)

## ABSTRACT

The mixel camera combines a new type of hardware component – an array of light mixing chambers – with a mathematical method that restores captured hyperspectral data with large keystone to its keystone-free form. When it is no longer necessary to correct keystone in hardware, the requirements to the optical design become much less stringent, and the mixel camera can therefore collect about four times more light than most traditional high-resolution cameras. However, for the mathematical data restoring method to function correctly, the geometry of the camera – such as the relative position of the image sensor and the slit – should be known with a small fraction of a pixel precision. Due to quite small sensor pixel size, it may be very challenging to make the camera so rigid mechanically that previously obtained calibration data remain valid for a long enough period. We will in this paper show how the captured hyperspectral data from the scene of interest, i.e., an unknown natural scene, can be used to give sufficiently precise calibration.

## INTRODUCTION

Hyperspectral cameras are increasingly used for various military, scientific, and commercial purposes. Push-broom cameras are particularly popular when high spatial and spectral resolution in combination with high signal-to-noise ratio is required. Unfortunately, these cameras also introduce spatial and spectral artefacts, known as keystone and smile, to the recorded hyperspectral data (1). This may significantly distort the captured spectra.

Smile could in principle be handled by oversampling the spectrum, since typically there are significantly more pixels on the sensor in the spectral direction than the required number of spectral channels. However, in the spatial direction one normally wants to take advantage of the full resolution of the sensor, and the problem with keystone can therefore not be handled the same way.

The mixel camera solves the problem with keystone by combining a new type of hardware component – an array of light mixing chambers – with a mathematical method to restore captured data with large keystone to its preferred keystone-free form (2,3). When it is no longer necessary to correct keystone in hardware, the optical design task becomes very much easier. This opens up for the possibility to design hyperspectral cameras that can collect at least four times more light than the widely used Offner design. An example of an optical system with high spatial resolution and light throughput, designed for a mixel camera, is shown in (2).

For the mathematical data restoring method to function correctly, the geometry of the camera (such as the relative position of the image sensor and the slit) should be known with a small fraction of a pixel precision. However, due to quite small sensor pixel size, it may be very challenging to make the camera so rigid mechanically that previously obtained calibration data remain valid for a long enough period. We will show that the captured data from the scene of interest, i.e., an unknown natural scene, can be used to give sufficiently precise calibration.

Norwegian and international PCT patent applications have been filed for the technology presented in this article (4,5). A prototype camera has been built and is currently being tested.

**THE MIXEL CAMERA CONCEPT**

We will first briefly describe the mixel camera concept. A more thorough description of the concept can be found in (2). The mixel camera contains a new type of hardware component – an array of light mixing chambers – that is inserted into the camera slit. Each chamber sees a particular area of the scene, and such an area is referred to as a ‘scene pixel’. The purpose of the chambers is to mix the incoming light from the scene pixels as evenly as possible, so that the light distribution at the output of a chamber becomes uniform and independent of the light distribution of the corresponding scene pixel, see Figure 1.

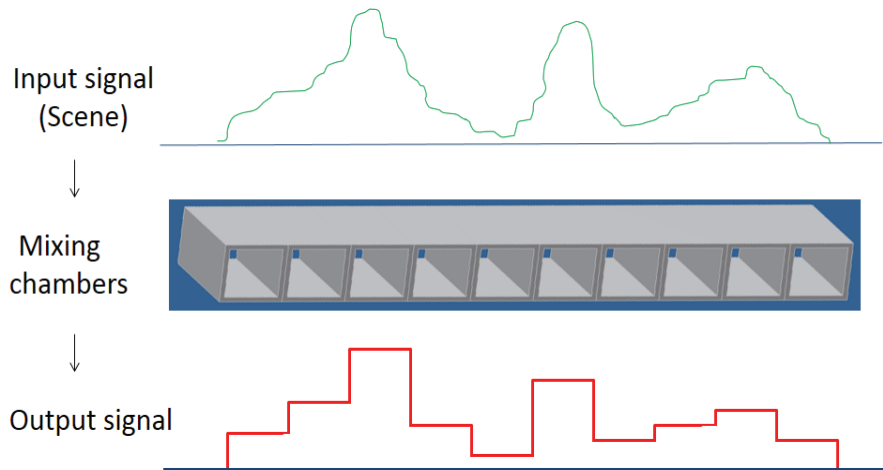


Figure 1: An example of how the light mixing chambers may look (only a few chambers are shown). The input signal from the scene (green curve) is mixed in the chambers so that the light distribution at the output of each chamber (red curve) becomes uniform.

The projection of a scene pixel onto the slit, as it appears after passing through the mixing chamber, is referred to as a ‘mixel’. The light content of a mixel is equal to the light content of the corresponding scene pixel, but while the light distribution over the scene pixel is *unknown* (due to subpixel sized details), the light distribution over the corresponding mixel is always *known* (uniform). When the light distribution is known, it is possible to restore data captured with keystone to its original keystone-free form.

In order to restore  $N$  mixels from  $M$  recorded sensor pixels, where  $M > N$ , we must utilize the data restoring equation set given in (2):

$$E_m^R = \sum_{n=1}^N q_{mn} E_n, \quad m = 1, 2, \dots, M \tag{1}$$

where  $E_n$  is the unknown value (energy) for mixel # $n$ ,  $E_m^R$  is the pixel value (energy) recorded in sensor pixel # $m$ , and  $q_{mn}$  is the fraction of the energy contained within mixel # $n$  that contributes to the value (energy) recorded in sensor pixel # $m$ . The coefficients  $q_{mn}$  depend on the keystone<sup>1</sup> and point-spread function (PSF) of the system, and are measured during camera calibration/characterization. Typically, only two scene pixels contribute to each recorded sensor pixel, therefore most of the coefficients  $q_{mn}$  are equal to zero. Keystone for different wavelengths relative to each other within one spectral channel is assumed to be negligible.

Note that the system has more equations than unknowns ( $M > N$ ). In fact, each extra pixel of keystone gives one extra equation. For the ideal case when there is no noise in the system, the

<sup>1</sup> Keystone is normally defined as a difference in position of a given scene pixel as it is depicted in two or more different spectral channels. In this paper, keystone is defined as the difference in position of a given scene pixel as it is depicted by a single spectral channel compared to a reference. For a camera where keystone is corrected in hardware, the reference is another spectral channel. For the mixel camera, the reference is the mixel array, i.e., if  $N$  mixels are imaged onto  $N+k$  sensor pixels for a given spectral channel, then this spectral channel has  $k$  pixels keystone.

equation system is compatible, i.e., can be solved. However, for a real system with noise, the system is overdetermined and an optimization method, such as for instance the least squares method, could be used to obtain the solution.

The restoring process described here corrects keystone and *PSF* differences in the optics between the slit and the sensor. The foreoptics, which images the scene onto the input of the mixing chamber array, still needs to be keystone free. However, the design of such foreoptics can be a relatively straightforward task, because (unlike the relay optics) the foreoptics of a hyperspectral camera is not required to disperse light spectrally. If the foreoptics only consists of reflective elements, then the rays of all wavelengths will follow precisely the same path, and keystone does not appear. Of course, the design and especially the alignment of very fast (i.e. low *F*-number) reflective foreoptics can be very difficult. Fortunately, the foreoptics itself can have a relatively high *F*-number even if the camera as a total is designed to have a low *F*-number. Keystone-free foreoptics can therefore utilise a relatively simple full reflective design such as a 3-mirror anastigmat. The field of view of such optics can be quite large – tens of degrees if necessary.

The restoring process can be repeated for all spectral channels, converting all the recorded data (with different keystone for different spectral channels) to the same final grid. No blur or misregistration errors are introduced to the data (as would have been the case if resampling was used for the conversion (6)). The result is a keystone-free hyperspectral image of the scene.

## CAMERA PERFORMANCE AND THE NEED FOR CALIBRATION

The mixel camera has been shown to have the potential to significantly outperform traditional cameras that correct keystone in hardware (2). However, this level of high performance requires that the camera is precisely calibrated. Below we will show how a shift in the relative position between the mixel array and the sensor pixels affects the camera performance, if the shift is not accounted for.

A Virtual Camera software (7) specifically developed for this purpose is used to simulate the mixel camera. The virtual camera uses the hyperspectral data of a real scene as input. The input data is somewhat distorted in accordance with the modeled optical distortions, sensor characteristics, and photon noise, giving a realistic picture of the size of the errors involved. Geometric ray-tracing is used to model the light mixing in the mixing chambers.

A hyperspectral data set containing 1600 spatial pixels, originally captured using a HySpex VNIR1600 hyperspectral camera (<http://www.hyspex.no/products/hyspex/vnir1600.php>), forms the “continuous” 1-dimensional scene (blue curve in Figure 2) to be captured by the virtual camera. The virtual camera is set to have significantly lower resolution (320 pixels) than the resolution of the scene. This means that five spatial pixels from the HySpex VNIR1600 data set form one scene pixel. By doing this, we simulate the fact that any real scene contains smaller details than the resolution of the camera being tested. The mixel camera is modelled to have 32 pixels keystone, i.e., the 320 scene pixels (or mixels) are recorded onto 352 sensor pixels.

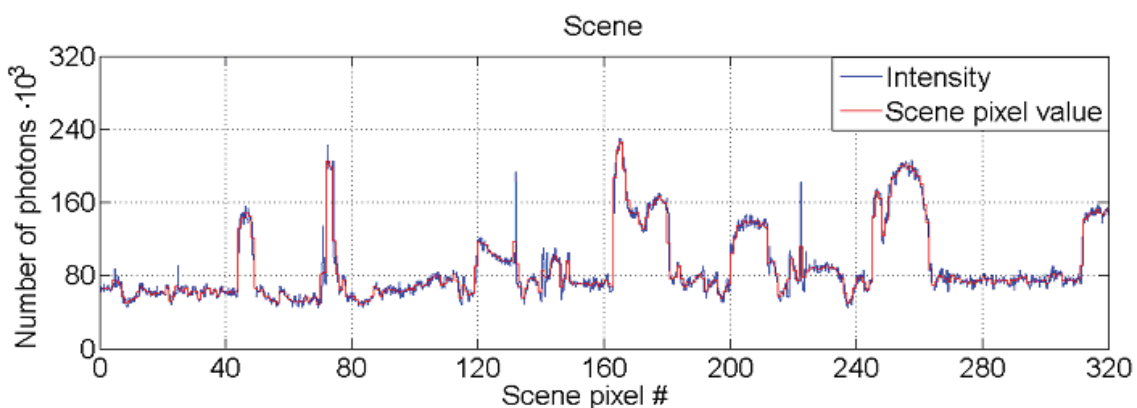


Figure 2: The reference scene consisting of 320 pixels. The blue curve shows the photon number density, while the red curve shows the corresponding scene pixel values.

When analysing the camera performance we look at the relative error,  $dE$ , given by:

$$dE = \frac{(E_{final} - E_{init})}{E_{init}} \tag{2}$$

where  $E_{init}$  is the scene pixel value (number of photons) and  $E_{final}$  is the calculated value of the same scene pixel after the signal has been processed by the camera.

Figure 3 shows the performance of the mixel camera when the camera is perfectly calibrated. Photon noise is included in the calculations. The standard deviation of the errors is 0.5% and the maximum error is 1.7%. The errors are not linked to any signal features and appear completely random. At this signal level, the camera is limited only by photon noise.

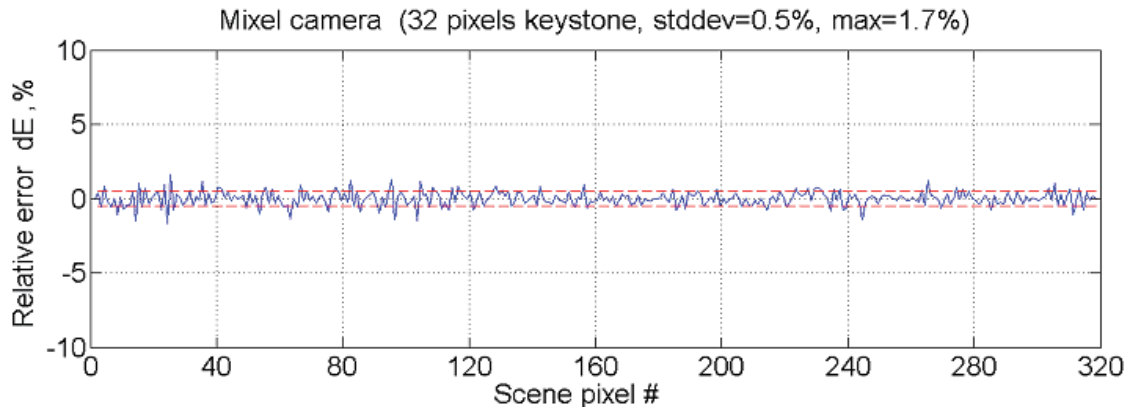


Figure 3: Mixel camera performance when the camera is perfectly calibrated. Photon noise is included in the calculations. The standard deviation of the errors is marked by a dashed red line.

Figure 4 shows the performance of the mixel camera when there is a shift of 0.05 mixel in the relative position between the mixel array and the sensor pixels, that has not been accounted for during the calculations, i.e., the coefficients  $q_{mn}$  in equation (1) were not adjusted according to the new position of the mixel array relative to the sensor pixels. Photon noise is included. The standard deviation of the errors has now increased to 1.1% and the maximum error is 4.9%. This means that the errors have more than doubled compared to when the camera is perfectly calibrated. The largest errors appear in the areas where the scene changes rapidly (see Figure 2). This is as expected, since these are the areas where a shift in the relative position between the mixel array and the sensor pixels will affect the data restoring process the most.

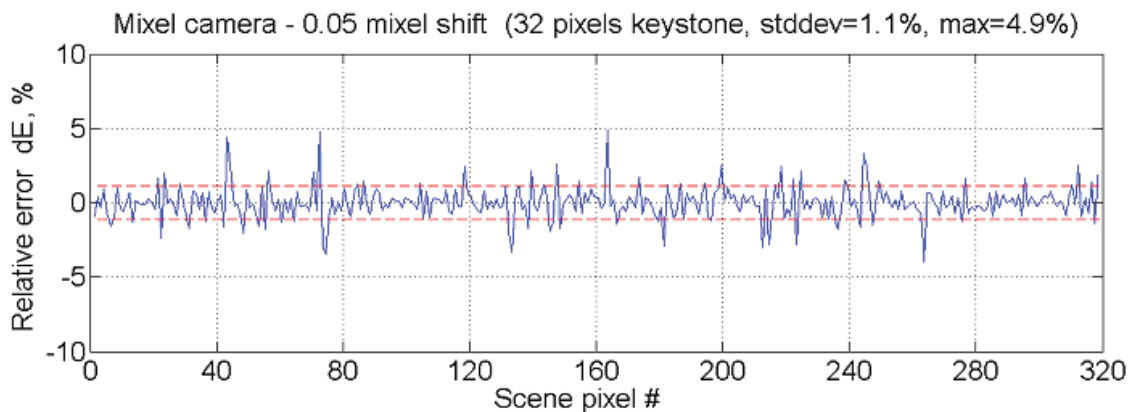


Figure 4: Mixel camera performance when there is a shift of 0.05 mixel in the relative position of the mixel array and the sensor pixels, that has not been accounted for. Photon noise is included in the calculations. The standard deviation of the errors is marked by a dashed red line.

The size of a mixel could typically be  $\sim 20 \mu\text{m}$  (2). A shift of 0.05 mixel then corresponds to a change in relative position between the mixel array and the sensor pixels of only  $1 \mu\text{m}$ , showing

clearly the need for very precise calibration of the camera. In the next section we will show how such precise calibration can be achieved.

### CALIBRATION BASED ON THE ACQUIRED HYPERSPECTRAL DATA

Solving the overdetermined equation system (1) will only provide correct mixel values if the coefficients  $q_{mn}$  are correct. These coefficients describe the geometry of the mixel array image on the sensor, as well as the PSF of the relay optics. Precise measurements of the coefficients  $q_{mn}$  can be obtained by adding two end mixels and a secondary mixel array to the slit (2). Here we will focus on the possibility to determine the coefficients in post-processing instead, based on the captured hyperspectral data.

Eq. (1) can be solved by use of the least squares method. This optimization method finds the solution  $\tilde{E}$  for the mixels that gives the best fit  $\tilde{E}^R$  to the recorded data  $E^R$ , i.e., the solution that minimizes the square sum of the mismatch errors  $\Delta$ :

$$\sum_{m=1}^M \Delta_m^2 = \sum_{m=1}^M (\tilde{E}_m^R - E_m^R)^2 \quad (3)$$

The more noise or other error sources that are present in the system, the more difficult it is to fit a solution, and the larger the mismatch errors will be. This fact can be used to calibrate the system with respect to the relative position between mixels and pixels, the relative length of the mixel array, and possibly also keystone and PSF, based only on the information in the captured image of a scene with unknown spatial and spectral content.

Imagine that the relative position between the mixel array and the sensor pixels has changed by a certain (unknown) amount. By solving the system of Eq. (1) for different assumed shifts in position and calculating the square sum of the mismatch errors in each case, we can find the actual position of the mixel array by choosing the assumed shift where the square sum is minimum.

Let us look at an example when the true shift in the relative position between the mixel array and the sensor pixels is  $x_0 = 0.150$  mixel. The input signal is the scene in Figure 3 and photon noise has been included in the calculations. Figure 5a shows the resulting mismatch errors when the shift in position has not been accounted for, i.e., when we have erroneously assumed that the shift is  $x = 0$  during the calculations. The mismatch errors are in this case large, approaching 3000 photons in some places. This means that the difference between the *measured* (recorded) sensor pixel value and the *calculated* value of the same sensor pixel (as found from the restored mixel values) can be as large as 3000 photons. The square sum of the mismatch errors was in this case found to be  $8.2 \cdot 10^7$ .

Figure 5b shows the resulting mismatch errors when we have made the correct assumption about the shift in relative position between the mixel array and the sensor pixels, i.e., when we have assumed that the shift is  $x = x_0 = 0.150$  mixel. The mismatch errors are now significantly smaller than in the previous case, indicating that our present assumption about the shift is more correct than the first assumption we made. The square sum of the mismatch errors is now reduced to  $3.2 \cdot 10^6$ .

If we calculate the square sum of the mismatch errors for many different assumed shifts, we get the curve shown in Figure 6. The curve for the square sum of the mismatch errors is found to have a minimum when the assumed shift is  $x_{min} = 0.154$  mixel (marked by red dashed line). This corresponds to an error in the determination of the shift of only  $\Delta x = 0.004$  mixel. Previous simulations have shown that the position of the mixel array relative to the sensor pixels should be known with an accuracy of  $\sim 0.01$  mixel or better (2). It seems clear that this requirement could be met by the suggested calibration method. If several spectral bands are used for the calibration, the accuracy could be increased further.

Figure 7 similarly shows an example of calibration of the relative length of the mixel array when the true length is  $L_0 = 352$  pixels, i.e., when the mixel array with 320 mixels covers 352 pixels on the sensor. The curve for the square sum is found to have a minimum when the assumed length is  $L_{min} = 352.002$  pixels (marked by red dashed line). The error in the determination of the mixel array length is then  $\Delta L = 0.002$  pixel. This corresponds to a maximum error of only  $dE = 0.1\%$  in the

restored input signal. The suggested calibration method therefore seems to work well also for determining the mixel array length.

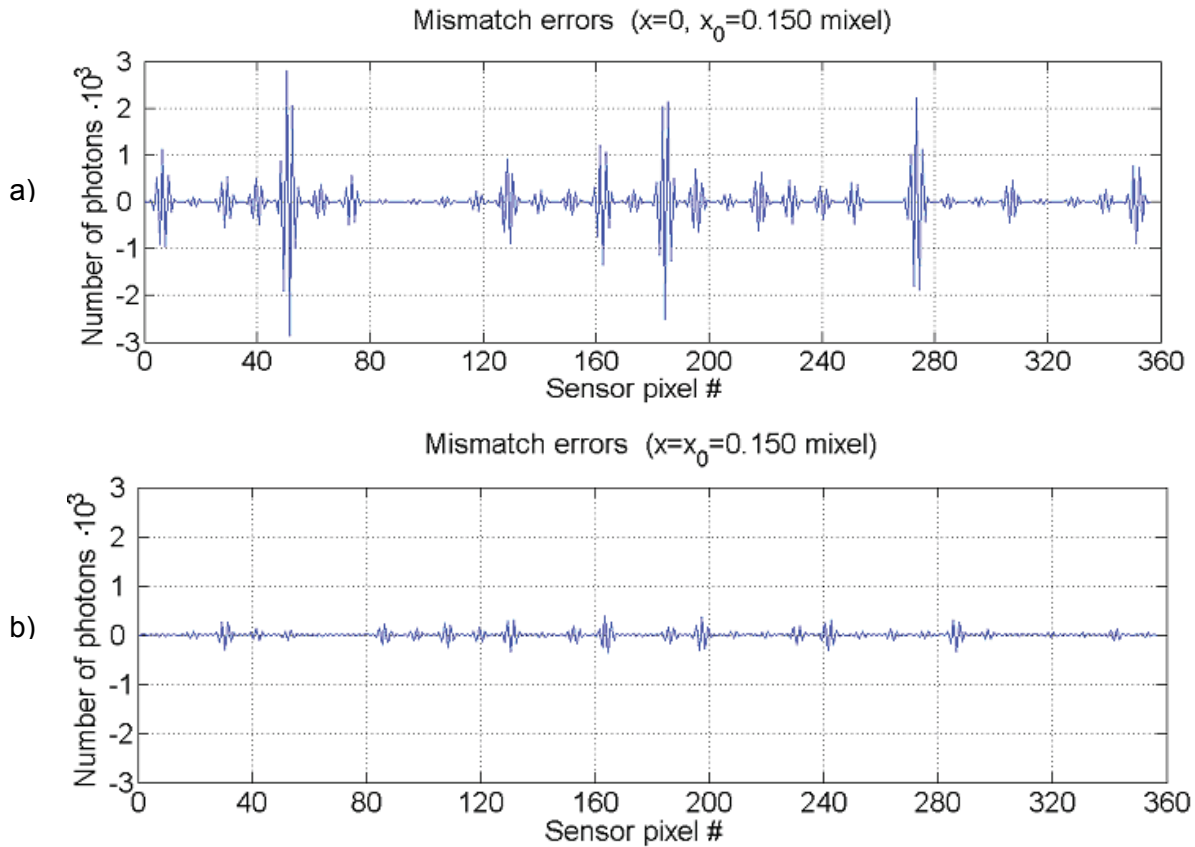


Figure 5: Mismatch errors when there is a shift of  $x_0=0.150$  mixel in the relative position between the mixel array and the sensor pixels. In a) no shift ( $x=0$ ) has been assumed during the calculations, while in b) the correct shift ( $x=x_0=0.150$  mixel) has been used. Photon noise has been included in the calculations.

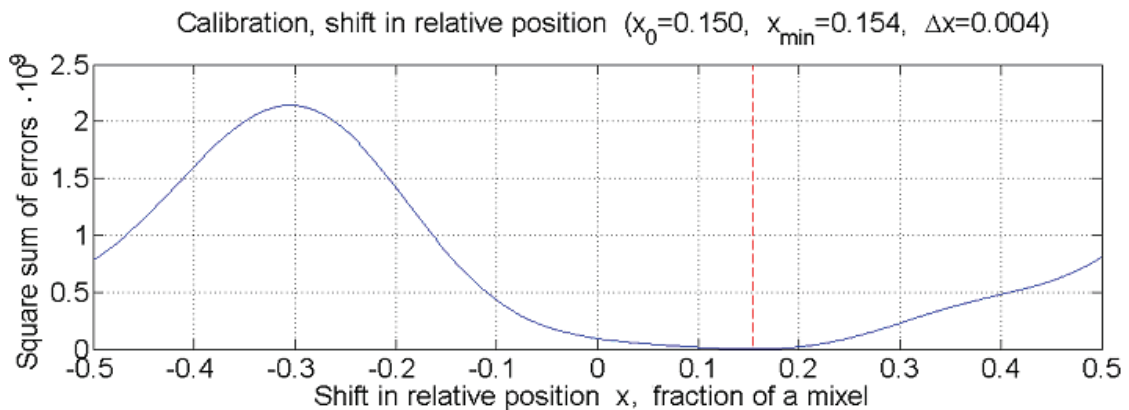


Figure 6: Square sum of the mismatch errors as a function of assumed shift  $x$  in relative position between the mixel array and the sensor pixels, when the true shift is  $x_0=0.150$  mixel. Photon noise has been included in the calculations.

So far, we have shown how the calibration method can be used to detect changes in the position and length of the mixel array relative to the sensor pixel array. These are the two most important cases to monitor. Small (submicron-to-micron) deformations are quite likely to appear in an instrument the size of a hyperspectral camera – causing changes in the relative position of the mixel array and the sensor. Similarly, variations in the temperature difference between these two camera elements may cause changes in their relative length. While the temperature changes are

relatively slow, the deformations of the camera mechanics may appear even on a frame-to-frame basis. This means that the amount of data available for finding the relative position of the mixel array is limited, since information from only a single frame can be used. On the other hand, the simulations in this section have shown that a single parameter (such as relative position or relative length of the mixel array) can be determined with sufficient precision based on a very limited amount of data: not only from a single frame, but also from a single spectral channel and very few mixels, if necessary.

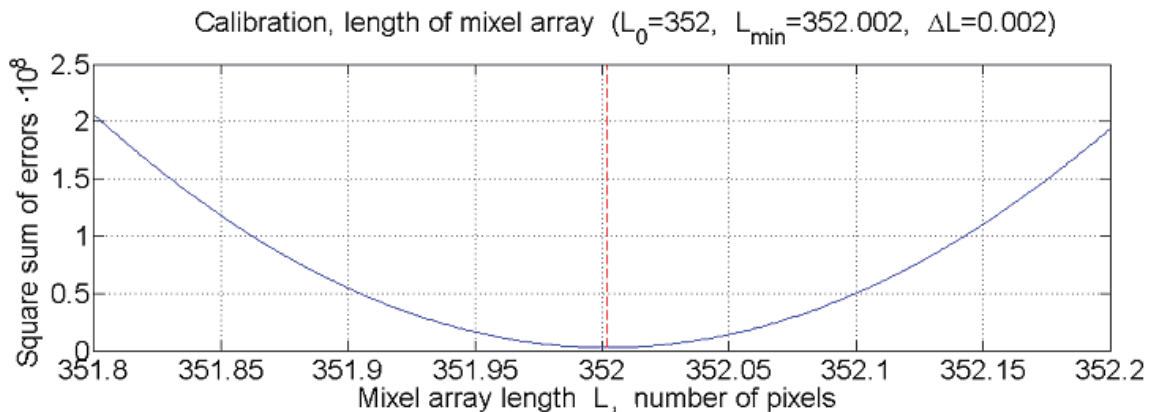


Figure 7: Square sum of the mismatch errors as a function of assumed mixel array length  $L$ , when the true length is  $L_0 = 352$  pixels. Photon noise has been included in the calculations.

The calibration method could possibly also be applied to monitor changes in keystone and *PSF*. Both change slowly across the field of view and wavelength range, and any drift with time will normally also be slow. In order to track the keystone and *PSF* changes several variables will have to be calculated, each describing the keystone or *PSF* width in a single field point for a single spectral channel. It may therefore be necessary to utilize several consecutive frames in order to obtain the required calibration precision.

The calibration method suggested here will give the best precision in the case of a scene with many small details (which is more or less any landscape or geological scene). On a scene with little spatial variation the results will be less precise. On the other hand, the restored image of the latter type of scene would have only relatively small errors even if the camera was poorly calibrated, precisely because of the absence of small high contrast details. In the case of low light (when photon noise is high compared to the signal), the situation will be somewhat similar: the described calibration method will be less precise, but due to the already higher errors in the system caused by the higher relative photon noise, a larger error in the calibration can be accepted without increasing the total errors of the system noticeably. In other words, this calibration method has a very useful property: it is more sensitive and works more precisely in situations where high precision is more important.

## CONCLUSION

The mixel camera delivers keystone-free hyperspectral images at high spatial resolution and can collect about four times more light than most traditional high-resolution cameras. However, the camera requires very precise calibration in order for the data restoring method to function correctly. A calibration method based on the captured data has been suggested, and has been shown to determine precisely the relative position between the mixel array and the sensor pixels as well as the relative length of the mixel array. The method could possibly also be used to determine changes in keystone and *PSF*.

## REFERENCES

- 1 Mouroulis P, R O Green & T G Chrien, 2000. Design of pushbroom imaging spectrometers for optimum recovery of spectroscopic and spatial information. Applied Optics, 39(13): 2210-2220
- 2 Høye G & A Fridman, 2013. [Mixel camera – a new push-broom camera concept for high spatial resolution keystone-free hyperspectral imaging](#). Optics Express, 21: 11057-11077
- 3 Høye G & A Fridman, 2009. A method for restoring data in a hyperspectral imaging system with large keystone without loss of spatial resolution. Forsvarets forskningsinstitutt, FFI-rapport 2009/01351, declassified on 28 January 2013
- 4 Høye G & A Fridman, 2013. Hyperspektralt kamera og metode for å ta opp hyperspektrale data. Norwegian patent application number 20111001
- 5 Høye G & A Fridman, 2013. Hyperspectral camera and method for acquiring hyperspectral data. PCT international patent application number PCT/NO2012/050132
- 6 Fridman A, G Høye & T Løke, 2013. Resampling in hyperspectral cameras as an alternative to correcting keystone in hardware, with focus on benefits for the optical design and data quality. In: Proc. SPIE 8706, Infrared Imaging Systems: Design, Analysis, Modeling, and Testing XXIV, 870602 (June 5, 2013)
- 7 Høye G & A Fridman, 2010. Performance analysis of the proposed new restoring camera for hyperspectral imaging. Forsvarets forskningsinstitutt, FFI-rapport 2010/02383, to be declassified